Matrix cracking and debonding of ceramic-matrix composites

François Hild, Alain Burr, Frederick A Leckie

MATRIX CRACKING AND DEBONDING OF CERAMIC–MATRIX COMPOSITES

FRANÇOIS HILD and ALAIN BURR
Laboratoire de Mécanique et Technologie, E.N.S. de Cachan/C.N.R.S./Université Paris 6, 61, Avenue du Président Wilson, F-94235 Cachan Cedex, France

and

FREDERICK A. LECKIE
Department of Mechanical and Environmental Engineering, University of California, Santa Barbara. CA 93106-5070. U.S.A.

Abstract—The effects of matrix cracking and debonding which occur in ceramic–matrix composites are described by a micromechanical model. The cracking and debonding processes induce loss of stiffness, inelastic strains, hysteresis loops and crack closure. These features are analysed within the framework of Continuum Mechanics by the introduction of internal variables identified in the micromechanical analysis. The evolution laws of the internal variables can be determined by combining the experimental data with micromechanical modeling. The influences of residual stress fields due to processing are also included. Comparisons are made between theoretical predictions and the results of experiments performed on layered materials.

1. INTRODUCTION

It is known that the formation of matrix cracks and the subsequent matrix–fiber interface sliding are the source of the nonlinear stress–strain curves observed when loading continuous fibers as well as ceramic–matrix composites. Matrix cracking and debonding reduce the secant Young's modulus $\bar{E}$, and induce inelastic strains upon complete unloading, $\bar{\varepsilon}_{in}$, and hysteresis loops, $\delta\bar{\varepsilon}$ (Beyerley *et al.*, 1992; Pryce and Smith, 1992).

In this paper, the effects of matrix cracking and interface sliding are studied within the framework of Continuum Damage Mechanics. Constitutive laws are derived by introducing internal variables which are identified in a micromechanical description of matrix cracking and debonding. The effects of residual stresses introduced during processing are also included. The growth laws for the internal state variables in terms of the associated forces are determined from experiments which involve unloading–reloading sequences. The procedures developed in the study are used to define a model which describes the tensile behavior of a layered laminate made of alternating layers of alumina and unidirectional carbon/epoxy prepreg tapes.

2. CONTINUUM MECHANICS FORMULATION

In this section, a Continuum Mechanics formulation (Germain, 1973; Lemaitre and Chaboche, 1985) is attempted using the framework of the thermodynamics of irreversible processes (Bataille and Kestin, 1979; Germain *et al.*, 1983). The first step in establishing such a model is to identify the internal state variables which define the condition of the material. The second is to determine the expression of the state potential in terms of the state variables and the third to define the evolution laws of the internal variables.

2.1. *Degradation mechanisms*

Upon loading, a composite or laminate which consists of a brittle matrix supported by a stronger material usually forms a pattern of multiple cracking. In fiber-reinforced systems and layered architectures, matrix cracking is usually accompanied by interfacial

debonding and sliding. At high values of stress, fiber breakage occurs which is accompanied by fiber pull-out and is mainly driven by the normal stresses or strains in the fiber directions (Hild *et al.*, 1994). These two mechanisms need different treatments.

Since the matrix cracking process occurs at load levels significantly lower than the fiber breakage mechanism, it is assumed that these mechanisms are uncoupled. The matrix cracks which normally occur at low values of stress are usually aligned with the principal stress or strain directions. These cracks cause stiffness reduction when the stress is tensile. In addition, it is the closure of the cracks which indicates the onset of increased stiffness when the specimen is subsequently loaded in compression. To be able to predict crack closure, the most natural choice of variable is the crack opening displacement Δ.

Debonding followed by sliding gives rise to inelastic strains and hysteresis loops. To model these phenomena, different models have been proposed (Cox, 1952; Aveston *et al.*, 1971; Hutchinson and Jensen, 1990; Hsueh, 1993). They all use an elementary cell of length $2L$, characterizing the average crack spacing, and consisting of two different materials (1) and (2), as shown in Fig. 1. There is a crack of size $2a$ at the center and a friction length $2l_F$. Thermal mismatch between parts (1) and (2) develops during processing. The self-balanced residual stress field is $-\rho_1 E_1/E$ and $-\rho_2 E_2/E$ in parts (1) and (2), respectively (Fig. 2), where E is Young's modulus of the unbroken composite, E_1 that of part (1) and E_2 that of part (2). When a crack appears, part of these residual stresses are relieved within the slipping region.

2.2. *State potential*

The model can describe the reduction in stiffness due to matrix cracking, the inelastic strains due to friction, the size of the hysteresis loops and the closure phenomenon when the loading is compressive. The details of the unloading and reloading process are fairly complex, but the introduction of the crack opening displacement Δ simplifies the calculations. To characterize the state of the composite, four different quantities are required. These are the overall strain $\bar{\varepsilon}$, the friction length $2l_F$, the cell length $2L$ and the crack opening displacement Δ. The expression of the strain distribution in the friction zone in part (2) is defined by a function F which depends on the details of the interfacial behavior, and is given by $\delta\varepsilon_2(z) = \delta\varepsilon_2 F(z)$, the difference between the strain field when friction occurs and the strain field with no friction, where z is the direction normal to the crack (Fig. 1). The crack opening displacement due to slip Δ_s is then given by

$$\Delta_s = \delta\varepsilon_2 l_F \frac{E}{fE_1} \bar{F}, \tag{1}$$

with

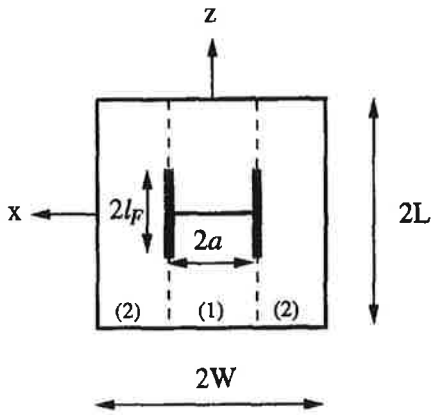

Fig. 1. Elementary cell of size $2L \times 2W$ containing a crack of size $2a$. A friction zone is characterized by a length $2l_F$.

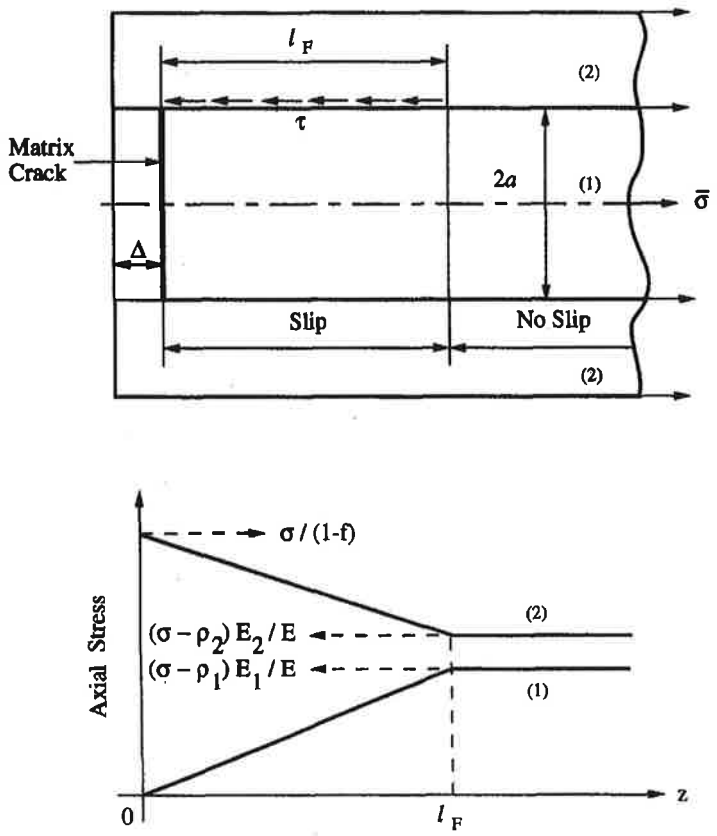

Fig. 2. Motion of the unbroken part (2) with respect to the broken part (1) with no external load by an amount Δ over a length l_F. Axial stresses in layers (1) and (2) with a constant shear strength.

$$\bar{F} = \frac{1}{l_F}\int_0^{l_F} F(z)\,dz,$$

where f is the volume fraction of part (1).

The free energy density for a given state is calculated by performing two elastic calculations. Two "cut and paste" steps are used to evaluate the elastic energies following approaches introduced by Volterra (1907), and used to analyse the elastic behavior of homogeneous and isotropic media by considering the elastic properties of a cut cylinder (Volterra, 1907; Love, 1927), as well as inclusions in an infinite medium (Eshelby, 1957), or to study creeping materials (Cocks and Leckie, 1987). The first step consists of calculating the elastic energy when the unbroken part (2) is moved with respect to the broken part (1) by an amount Δ_s over a length l_F (Fig. 2) with no external load. This displacement Δ_s gives rise to a self-balanced stress field along a length l_F in parts (1) and (2). By integration over l_F, and averaging over the total length L, the elastic energy density associated with this process is given by (see Appendix):

$$\psi_s = \frac{\Delta_s^2}{2Ll_F}\frac{fE_1(1-f)E_2}{E}\frac{\bar{F}}{\bar{F}^2}, \tag{2}$$

with

$$\bar{F} = \frac{1}{l_F}\int_0^{l_F} F^2(z)\,dz.$$

The crack opening displacement Δ_s induces an overall inelastic strain α due to slip, expressed as

$$\alpha = \frac{fE_1}{E}\frac{\Delta_s}{L}. \tag{3}$$

The second step consists of an elastic loading of a cracked system with friction prevented. The presence of a crack results in a stiffness reduction defined by an internal damage variable D (Budiansky and O'Connell, 1976; Chaboche, 1982), so that the elastic energy density is given by

$$\psi_e = \tfrac{1}{2}E(1-D)(\bar{\varepsilon}-\alpha)^2. \tag{4}$$

This damage variable D depends upon the crack density $\pi a^2/4LW$, as well as the elastic properties of the two components. In the following treatment, the exact microscopic description is not needed. The total free energy density is the sum of the two components of energy. For convenience the free energy can be expressed in a more compact form by using four state variables, which are the total strain $\bar{\varepsilon}$ and three internal variables, namely the damage variable D modeling the loss of stiffness due to the cracking mechanism, the damage variable $d = fE_1/(1-f)E_2 l_F/L$ which defines the size of the slip zone related to the crack spacing, and the inelastic strain α due to slip. The free energy density in terms of the new internal variables is

$$\psi = \tfrac{1}{2}E(1-D)(\bar{\varepsilon}-\alpha)^2 + \tfrac{1}{2}E^*\left(\frac{\alpha^2}{d}\right), \tag{5}$$

with

$$E^* = E\frac{\bar{F}}{\bar{F}^2}.$$

The crack opening strain α is similar to a kinematic hardening variable, since eqn (3) shows that the opening displacement Δ_s can be related to the inelastic strain, and the associated force corresponds to the back-stress induced by the slipping mechanism. The forces associated with the previous variables are respectively given by

$$\bar{\sigma} = \frac{\partial \psi}{\partial \bar{\varepsilon}} = E(1-D)(\bar{\varepsilon}-\alpha) \tag{6a}$$

$$Y = -\frac{\partial \psi}{\partial D} = \frac{E}{2}(\bar{\varepsilon}-\alpha)^2 \tag{6b}$$

$$y = -\frac{\partial \psi}{\partial d} = \frac{E^*}{2}\left(\frac{\alpha}{d}\right)^2 \tag{6c}$$

$$X = \frac{\partial \psi}{\partial \alpha} = -\bar{\sigma} + E^*\frac{\alpha}{d}. \tag{6d}$$

Equation (6a) can be rewritten in terms of a total crack opening which consists of the contribution of the elastic opening augmented by the opening due to slip

$$\bar{\varepsilon} - \frac{\bar{\sigma}}{E} = \frac{\bar{\sigma}D}{E(1-D)} + \alpha, \tag{7a}$$

so that the crack closure condition is given by

$$\frac{\sigma D}{E(1-D)}+\alpha=0. \tag{7b}$$

Lastly, the growth laws of the internal variables can be established from the results of materials science, but these in themselves can be major undertakings, as is evidenced by the work of Curtin (1991) describing the fragmentation process in a model where constant shear stress along the interface is assumed. This analysis requires substantial information about the statistical failure properties of part (1). Another method which is more practical and in keeping with the aim of this approach is to deduce the evolution of the state variables from experimental data.

2.3. *Evolution laws*

When deriving the expressions for the elastic energy it was not necessary to have precise information about the conditions of slip and/or debond properties of the fiber–matrix interface. To proceed further it is necessary to have information about the interface and in the following it is assumed that the stress of the interface has a constant value τ, over the friction length l_F. It can be shown that $\delta\varepsilon_2 = f\tau/(1-f)E_2$, $F(z) = (l_F - z)/a$, so that $\bar{F} = l_F/2a$, $\bar{\bar{F}} = l_F^2/3a^2$ and $E^* = 4E/3$.

It will be demonstrated that the evolution laws can be deduced from the measurements during a loading–unloading–reloading sequence. Reversed motion of fibers relative to the matrix has been studied by numerous authors (Marshall and Oliver, 1987; McMeeking and Evans, 1990; Pryce and Smith, 1992). The main results are now summarized. After reaching a maximum stress value σ_M, when the maximum friction length is l_{FM}, the load is reversed (Fig. 3). Upon unloading by $\delta\sigma_U$, in the range $0 \leqslant |z| \leqslant l_{FU}$, where l_{FU} is the unloading friction length, both the relative sliding direction and the frictional shear stress reverse. Between $l_{FU} \leqslant |z| \leqslant l_{FM}$, the shear stress remains unchanged from that prevailing during the loading process. After reaching a minimum value of stress when $\delta\sigma_U = \sigma_m$, the load is reversed again (Fig. 3), causing reloading. Upon reloading by $\delta\sigma_R$, sliding is confined to $0 \leqslant |z| \leqslant l_{FR}$. The expression for total strain is

$$E\bar{\varepsilon} = (\sigma_M - \sigma_m + \delta\sigma_R) + \frac{fE_1}{(1-f)E_2}\frac{l_{FM}}{L}\frac{2(\sigma_M-\rho_1)^2-\sigma_m^2+\delta\sigma_R^2}{4(\sigma_M-\rho_1)} \tag{8a}$$

and the crack opening displacement due to slip during the sequence is given by

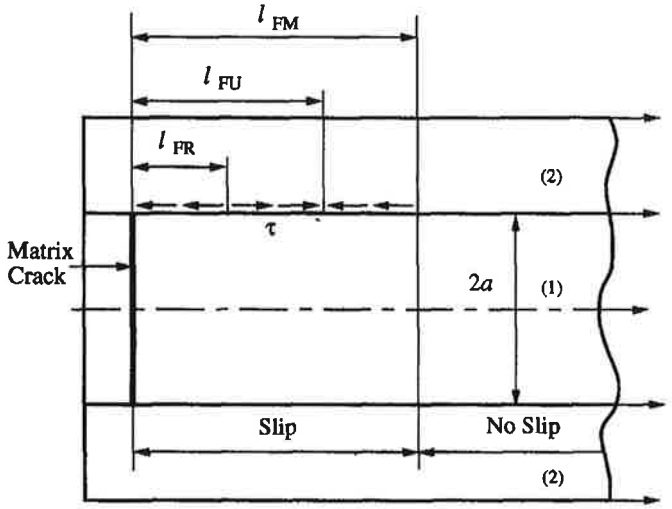

Fig. 3. Depiction of the friction length, l_F upon loading, the unloading friction length, l_{FU}, and the reloading friction length, l_{FR}.

$$\Delta_s(\sigma_M, \sigma_m, \delta\sigma_R) = \frac{l_{FM}}{(1-f)E_2} \frac{2(\sigma_M-\rho_1)^2-\sigma_m^2+\delta\sigma_R^2}{4(\sigma_M-\rho_1)}. \tag{8b}$$

The crack opening displacement Δ_s is also related to the total strain by

$$\bar{\varepsilon} - \frac{fE_1}{E}\frac{\Delta_s}{L} = \frac{\sigma}{E}. \tag{9}$$

For a cracked system, a loss of stiffness is involved. The effect of this change of Young's modulus can also be interpreted in terms of effective stress (Rabotnov, 1963; Lemaitre and Chaboche, 1978). The microscopic or "effective" stress, $\sigma = \bar{\sigma}/(1-D)$, is higher than the macroscopic stress $\bar{\sigma}$ because of the presence of a crack. Therefore, the stress–strain relationship becomes

$$\bar{\varepsilon} - \alpha = \frac{\bar{\sigma}}{E(1-D)}. \tag{10}$$

Equation (10) is consistent with eqn (6a). Upon loading, the evolution of the irreversible strain α is given by

$$\alpha = \frac{d}{2}\frac{\bar{\sigma}_M - \rho_1(1-D)}{E(1-D)}. \tag{11a}$$

The variation of α, $\delta\alpha = \alpha - \alpha_0$, with respect to minimum or maximum value, α_0 (corresponding to a maximum loading or minimum unloading level characterized by $\bar{\sigma}_0$) is related to the stress variation, $\delta\bar{\sigma} = \bar{\sigma} - \bar{\sigma}_0$, by

$$\delta\alpha = \frac{d}{4}\frac{(\delta\bar{\sigma})^2}{E(1-D)[\bar{\sigma}_M - \rho_1(1-D)]}\,\mathrm{Sign}\,(\delta\bar{\sigma}). \tag{11b}$$

Instead of tracking the complicated pattern of friction and reverse friction, it is found to be convenient to introduce the opening strain into the calculations.

The expression of the maximum hysteresis loop width, $\delta\bar{\varepsilon}$, is given by

$$\delta\bar{\varepsilon} = \frac{d}{4}\frac{\bar{\sigma}_M^2}{2E(1-D)[\bar{\sigma}_M - \rho_1(1-D)]}. \tag{12}$$

Equation (12) shows the role of residual stresses on the evolution of the maximum hysteresis loop width. When the residual stresses vanish, a simple relationship exists between the inelastic strain and the maximum hysteresis loop width (Fig. 4):

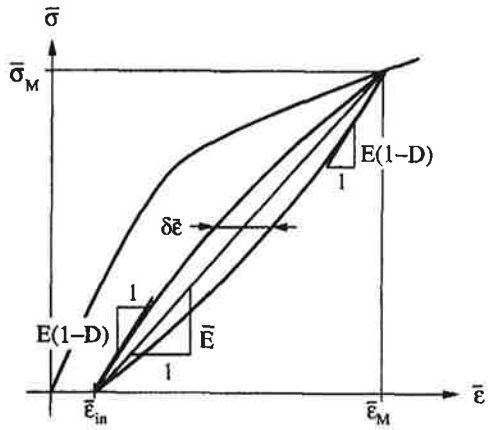

Fig. 4. Stress, $\bar{\sigma}$, versus strain, $\bar{\varepsilon}$, during a loading–unloading–reloading sequence.

$$2\delta\bar{\varepsilon} = \bar{\varepsilon}_{in}, \tag{13}$$

where $\bar{\varepsilon}_{in}$ is equal to α when $\bar{\sigma}_m = 0$. When $\bar{\sigma}_m = 0$, the inelastic strains are given by

$$\bar{\varepsilon}_{in} = \frac{d}{4}\frac{2[\bar{\sigma}_M - \rho_1(1-D)]^2 - \bar{\sigma}_M^2}{E(1-D)[\bar{\sigma}_M - \rho_1(1-D)]} \tag{14}$$

and the macroscopic closure stress, reached when $\bar{\sigma} = \bar{\sigma}_c$, is given by solving eqn (7b):

$$\frac{\bar{\sigma}_c}{\bar{\sigma}_M} = \left\{1 - \frac{2D}{d}[\bar{\sigma}_M - \rho_1(1-D)]\left[1 + \left(1 + \frac{d}{D}\frac{\bar{\sigma}_M}{\bar{\sigma}_M - \rho_1(1-D)} + \frac{d^2}{2D^2}\right)^{1/2}\right]\right\}. \tag{15}$$

Equation (15) defines the role of the residual stress field but as the damage parameter D increases, the effect of the initial residual stress field becomes less important. Furthermore, when the damage parameter d is very small (i.e. τ is large), the closure condition is given by $\bar{\sigma}_c \approx 0$, and the elastic strains are small as well (therefore $\bar{\varepsilon}_c \approx 0$).

Equations (11)–(15) are only valid when saturation is not reached. Beyond that point, these evolution laws need to be altered in order to account for matrix cracking saturation ($L = l_F$). Lastly, a means of determining the variable D is to measure the initial unloading modulus, which is equal to $\tilde{E} = E(1-D)$. Similarly, the initial reloading modulus is equal to $\tilde{E} = E(1-D)$, as shown in Fig. 4.

2.4. *Identification from macroscopic quantities*

By using eqn (6a) and the definitions of the internal variables, it is possible to measure some of the internal variables macroscopically. To get the necessary additional information, a complete loading–unloading–reloading sequence is needed. The useful information is the maximum applied strain $\bar{\varepsilon}_M$, the inelastic strain corresponding to a complete unloading $\bar{\varepsilon}_{in}$, the maximum hysteresis loop width $\delta\bar{\varepsilon}$ and the macroscopic Young's modulus $\tilde{E} = E(1-\bar{D})$ shown in Fig. 4. Three state variables, $\bar{\varepsilon}_M$, $\bar{\varepsilon}_{in}$ and $\bar{D}$, can be used in a phenomenological model where it is assumed that the unloading process is linear (Fig. 4). The expression of the corresponding state potential $\bar{\psi}$ is written as (Lemaitre and Chaboche, 1985)

$$\bar{\psi} = \tfrac{1}{2}E(1-\bar{D})(\bar{\varepsilon} - \bar{\varepsilon}_{in})^2. \tag{16}$$

The stress is obtained by partial differentiation of $\bar{\psi}$ with respect to the total strain $\bar{\varepsilon}$:

$$\bar{\sigma} = \frac{\partial\bar{\psi}}{\partial\bar{\varepsilon}} = E(1-\bar{D})(\bar{\varepsilon} - \bar{\varepsilon}_{in}), \tag{17a}$$

and the forces associated with the inelastic strain $\bar{\varepsilon}_{in} = \alpha(\bar{\sigma} = 0)$, and with the macroscopic damage $\bar{D}$, are respectively given by

$$\bar{\sigma} = -\frac{\partial\bar{\psi}}{\partial\bar{\varepsilon}_{in}} \tag{17b}$$

$$\bar{Y} = -\frac{\partial\bar{\psi}}{\partial\bar{D}} = \tfrac{1}{2}E(\bar{\varepsilon} - \bar{\varepsilon}_{in})^2. \tag{17c}$$

Within the framework of Continuum Damage Mechanics, $\bar{Y}$ is the strain energy release rate density (Chaboche, 1978). In this study, the evolution of the two internal variables $\bar{\varepsilon}_{in}$ and $\bar{D}$ is obtained from experiments by plotting their evolution against the respective associated forces, which are assumed to be the driving forces. The measurement of the inelastic strains is easy to carry out since it involves complete unloading. The measurement

of the damage variable can be performed through the measurement of the unloading modulus $\bar{E} = E(1-\bar{D})$.

In this approach the internal variables are obtained from macroscopic measurements. Since the residual stresses are unknown but constant, additional information is needed to evaluate them, i.e. the maximum hysteresis loop width $\delta\bar{\varepsilon}$. From the knowledge of the four previous quantities, the expressions for the damage variables are given by

$$D = \frac{\bar{\varepsilon}_M \bar{D} - \bar{\varepsilon}_{in}\bar{D} - 2\delta\bar{\varepsilon}}{\bar{\varepsilon}_M - \bar{\varepsilon}_{in} - 2\delta\bar{\varepsilon}} \tag{18a}$$

$$\frac{d}{4} = \frac{\sqrt{(\bar{\varepsilon}_{in} + 2\delta\bar{\varepsilon})\delta\bar{\varepsilon}}}{\bar{\varepsilon}_M - \bar{\varepsilon}_{in} - 2\delta\bar{\varepsilon}} \tag{18b}$$

and the residual stress in part (1) is

$$\frac{-\rho_1}{E} = \left(\sqrt{\frac{\bar{\varepsilon}_{in} + 2\delta\bar{\varepsilon}}{4\delta\bar{\varepsilon}}} - 1\right)(\bar{\varepsilon}_M - \bar{\varepsilon}_{in} - 2\delta\bar{\varepsilon}). \tag{18c}$$

Equations (18) allow us to quantify the microscopic variables by using macroscopic quantities. To complete the evolution laws, the driving forces need to be known. For the damage variable D, the natural driving force is its associated force Y. The role played by Y is similar to that played by the energy release rate $\mathcal{G}$ in Linear Elastic Fracture Mechanics. Similarly, the driving force of the damage variable d is assumed to be its associated force y. Lastly, the force X associated with the inelastic strain can be its driving force. However, eqns (11) show that the macroscopic stress can also be taken and therefore will be chosen for the sake of simplicity.

In the following the previous results are applied to a layered material. It is, however, worth noting that these results can also be applied to fiber-reinforced systems. The definition of the damage variables and the opening strain may change slightly, but the essential features obtained in this paper are identical. In particular, the method of deriving the free energy density through two elastic steps can be conserved.

3. ANALYSIS OF EXPERIMENTS ON A LAYERED MATERIAL

The previous model will be used to predict the behavior of a layered material subject to tension. The material is constructed by alternating three alumina plates and two unidirectional carbon/epoxy prepreg tapes. The laminate is put in a Kapton vacuum bag at room temperature, then hot pressed at a moderate pressure of 350 kPa and at a temperature of 135°C for 90 min (Lange *et al.*, 1992; Sherman, 1992). The tensile stress–strain response is shown in Fig. 5. Because of the discrete process of matrix cracking, there are stress drops at each new break.

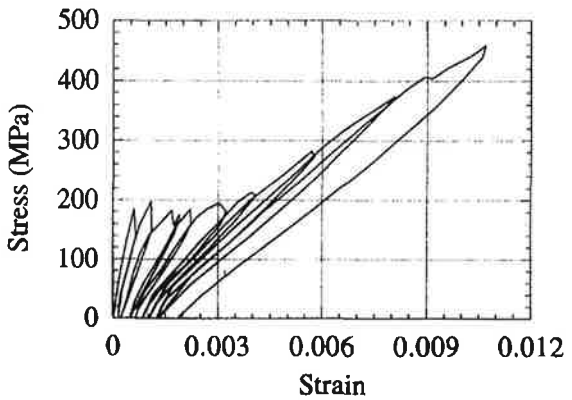

Fig. 5. Experimental stress–strain curve of a layered material subject to tension [after Sherman (1992)].

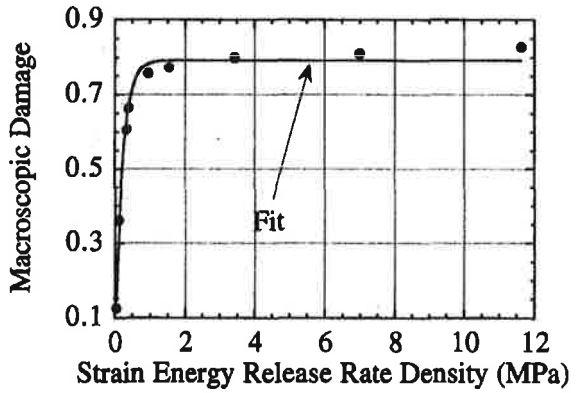

Fig. 6. Experimental and fitted evolution of the macroscopic damage variable as a function of strain energy release rate density.

This first part of the identification used macroscopic data only. The evolution of the macroscopic damage $\bar{D}$ and the inelastic strains ε_{in} are plotted against their respective associated forces, $\bar{Y}$ and $\bar{\sigma}$. The evolution of the macroscopic damage $\bar{D}$ against the associated force $\bar{Y}$ is shown in Fig. 6. The damage variable saturates so that a convenient way of describing this growth law is the exponential form

$$\bar{D} = \bar{D}_\infty \left\{ 1 - \exp\left(- \frac{\bar{Y}}{\bar{Y}_1} \right) \right\}. \tag{19}$$

The parameter $\bar{D}_\infty$ corresponds to the saturation value of the macroscopic damage $\bar{D}$ and $\bar{Y}_1$ is a normalizing strain energy release rate density. For this particular system the following values are obtained:

$$\begin{aligned} \bar{D}_\infty &= 0.79 \pm 0.01 \\ \bar{Y}_1 &= 0.21 \pm 0.02 \end{aligned} \tag{20}$$

Figure 7 shows the evolution of the inelastic strain as a function of the applied stress $\bar{\sigma}$. A third order polynomial describes well the experimental measurements

$$\varepsilon_{in} = \varepsilon_0 + \frac{\bar{\sigma}}{S_1} - \left(\frac{\bar{\sigma}}{S_2} \right)^2 + \left(\frac{\bar{\sigma}}{S_3} \right)^3, \tag{21}$$

with

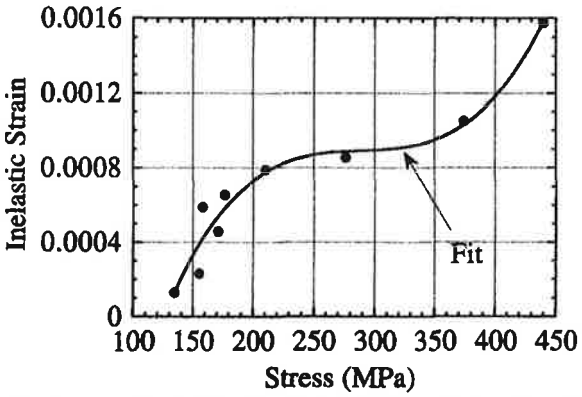

Fig. 7. Experimental and fitted evolution of the inelastic strain as a function of stress.

$$\varepsilon_0 = -0.003 \pm 0.001$$
$$S_1 = 21 \pm 6\,\text{GPa}$$
$$S_2 = 2.4 \pm 0.4\,\text{GPa}$$
$$S_3 = 1.7 \pm 0.2\,\text{GPa}. \tag{22}$$

The agreement between experiments and identification is good in terms of stress–strain response as well. The identifications performed in this subsection constitute the basis of the identification of the microscopic model. So far, the identification consists of choosing the type of function describing the experiments, and of fitting the parameters of each function.

In the following, the evolution laws of the microscopic quantities, namely the damage measures of d and D, the inelastic strain α and the residual stress $-\rho_1$ will be determined. The residual stress is important since it defines the onset of the first matrix crack in a composite system (Budiansky *et al.*, 1986). The first step is to compute the residual stress $-\rho_1$. By using eqn (18c), and the experimental data concerning $\bar{\varepsilon}_M$, $\bar{\varepsilon}_{in}$ and the maximum hysteresis loop width, $\delta\bar{\varepsilon}$, the residual stress $-\rho_1$ can be calculated at each experimental data point. It is found that the value of $-\rho_1$ varies, and since the residual stress is constant, the average for $-\rho_1$ is identified to be a tensile stress of $+18$ MPa (i.e. a residual stress of the order of 25 MPa). This value is consistent with independent observations by removing one alumina layer that found a tensile residual stress of the order of 20 MPa in the alumina layer (Sherman, 1992). It is worth remembering that the basis of identification of the residual stresses is such that saturation is not observed macroscopically (i.e. the damage variable still increases).

Since $\bar{D}$ and $\bar{\varepsilon}_{in}$ are easy to measure, these measurements will be used to establish their evolution laws as a fit of those experimental data. By using eqn (18c), the evolution law of the maximum hysteresis loop width, $\delta\bar{\varepsilon}$, is then completely known and given by

$$2\delta\bar{\varepsilon} = \bar{\varepsilon}_{in}\,\frac{1}{2\left[1+\dfrac{-\rho_1}{E(\bar{\varepsilon}_M-\bar{\varepsilon}_{in}-2\delta\bar{\varepsilon})}\right]^2-1}. \tag{23}$$

Figure 8 shows the comparison between the experiments and the predictions; the agreement is good. These results are compared with those obtained when residual stresses are assumed to be negligible and correspond to the dashed lines in Fig. 8. In that case, eqn (13) applies and leads to an overestimate of the maximum hysteresis loop width. The knowledge of the parameter $-\rho_1$ is therefore crucial to the evolution of the maximum hysteresis loop width and the inelastic strain.

The values of the damage variables can be determined by using eqns (18a, b). Measuring the initial unloading Young's modulus gives directly the value of D, which can be compared with the prediction. Figure 9 shows the comparison between the experiments

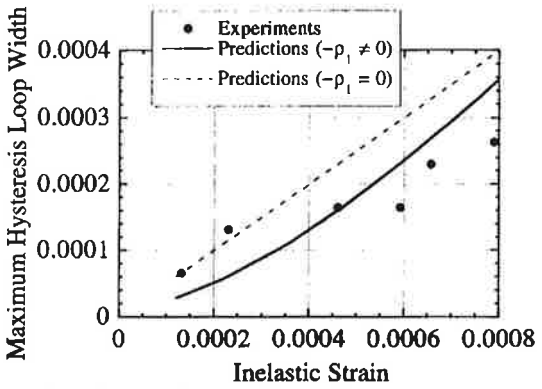

Fig. 8. Experimental and predicted evolution of the maximum hysteresis loop width as a function of inelastic strain, when $-\rho_1 = 0$ MPa and $-\rho_1 = 18$ MPa.

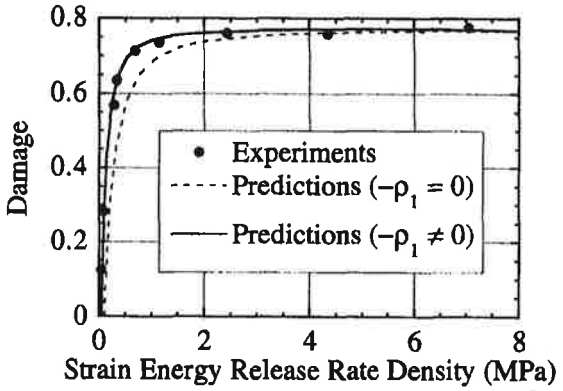

Fig. 9. Experimental and predicted evolution of the damage variable D as a function of strain energy release rate density Y, when $-\rho_1 = 0$ MPa and $-\rho_1 = 18$ MPa.

and the predictions; the agreement is very good. These results are again compared to those obtained when the residual stresses can be neglected. In this case there is a slight change in the initial unloading Young's modulus, measured by the damage variable D; this change disappears as D increases. The residual stresses have a weak effect on the damage variable D, modeling the change of stiffness due to matrix cracks. Unfortunately, there is no direct way of comparing the damage variable d obtained experimentally and numerically. Equation (15) shows that the knowledge of the damage variable d is crucial to compute the crack closure stress, as well as the saturation condition ($L = l_F$).

4. CONCLUSIONS

A micromechanical model is derived to describe loading and unloading sequences. These sequences induce slip and reverse slip. Because of friction, permanent strains appear upon complete unloading. Moreover, hysteresis loops are observed upon unloading and reloading. These hysteresis loops characterize the amount of energy that is dissipated during one unloading–reloading cycle. A convenient means of characterizing the sequences is to introduce the crack opening displacement between broken and unbroken parts.

A model based upon microscopic variables is formulated within a framework of Continuum Damage Mechanics. This model uses four state variables, one observable variable, i.e. the total strain, and three internal variables, namely two damage variables on a microscopic level which are matrix cracking and interface debonding, and crack opening strains proportional to the opening displacement due to slip divided by the average crack spacing. The free energy can be calculated in terms of these state variables, from which the associated forces can be derived. The identification procedure to determine the evolution laws uses measurements obtained from loading–unloading–reloading sequences. The macroscopic damage, inelastic strain and maximum hysteresis loop width, used in the identification procedure, are easy to measure experimentally. These quantities can also be used to calculate the residual stresses.

The procedures were applied to experiments performed on an alumina–carbon/epoxy prepreg layered material. The predictions in terms of hysteresis loop width and initial unloading Young's modulus agree well with the experiments. It is shown that the residual stress field has a strong influence on the evolution of the inelastic strains and the maximum hysteresis loop width. On the other hand, the evolution of the initial unloading Young's modulus is weakly affected by the residual stress field. This model was able to capture all the details of the microscopic study with only three internal variables.

This model will constitute the basis of a constitutive law applied to ceramic–matrix composites subject to complex loading conditions. In particular, the knowledge of the free energy density, the internal variables and their associated forces are crucial. These laws need to be generalized under more complex loading conditions.

Acknowledgements—This work was supported by the Defense Advanced Research Project Agency through the University Research Initiative under Office of Naval Research Contract No. N-00014-92-J-1808.

REFERENCES

Aveston, J., Cooper, G. A. and Kelly, A. (1971). Single and multiple fracture. In *Conference Proceedings of the National Physical Laboratory: Properties of Fiber Composites*. IPC Science and Technology Press, Surrey, U.K.

Bataille, J. and Kestin, J. (1979). Irreversible processes and physical interpretations of rational thermodynamics. *J. Non Equil. Thermodyn.* **4,** 229–258.

Beyerley, D., Spearing, S. M., Zok, F. W. and Evans, A. G. (1992). Damage, degradation and failure in a unidirectional ceramic–matrix composite. *J. Am. Ceram. Soc.* **75,** 2719–2725.

Budiansky, B., Hutchinson, J. W. and Evans, A. G. (1986). Matrix fracture in fiber-reinforced ceramics. *J. Mech. Phys. Solids* **34,** 167–189.

Budiansky, B. and O'Connell, R. J. (1976). Elastic moduli of a cracked system. *Int J. Solids Structures* **12,** 81–97.

Chaboche, J.-L. (1978). Description thermodynamique et phénoménologique de la viscoplasticité cyclique avec endommagement. Thèse de doctorat d'état, Université Paris 6.

Chaboche, J.-L. (1982). Le concept de contrainte effective appliquée à l'élasticité et à la viscoplasticité en présence d'un endommagement anisotrope. *Coll. Int. CNRS* **295,** 31–43.

Cocks, A. C. F. and Leckie, F. A. (1987). Creep constitutive equations for damaged materials. In: *Advances in Applied Mechanics* (Edited by J. W. Hutchinson and T. Y. Wu), Vol. 25, pp. 239–294. Academic Press, New York.

Cox, H. L. (1952). The elasticity and the strength of paper and other fibrous materials. *Br. J. Appl. Phys.* **3,** 72–79.

Curtin, W. A. (1991). Exact theory of fiber fragmentation in single-filament composite. *J. Mater. Sci.* **26,** 5239–5253.

Eshelby, J.D. (1957). The determination of the elastic field of an ellipsoidal inclusion and related problems. *Proc. R. Soc. Lond.* **A241,** 376–396.

Germain, P. (1973). *Cours de Mécanique des Milieux Continus*. Masson, Paris.

Germain, P., Nguyen, Q. S. and Suquet, P. (1983). Continuum thermodynamics. *J. Appl. Mech.* **50,** 1010–1020.

Hild, F., Burr, A. and Leckie, F. A. (1994). Fiber breakage and fiber pull-out of fiber-reinforced ceramic–matrix composites. *Eur. J. Mech. A/Solids* **13,** 731–749.

Hsueh, C.-H. (1993). Evaluation of interfacial properties of fiber-reinforced ceramic composites using a mechanical properties microprobe. *J. Am. Ceram. Soc.* **76,** 3041–3050.

Hutchinson, J. W. and Jensen, H. M. (1990). Models for fiber debonding and fiber pull-out in brittle composites with friction. *Mech. Mater.* **41,** 2365.

Lange, F. F., Marshall, D. B. and Folsom, C. F. (1992). U.S. Patent No. 5092948. University of California, Santa Barbara.

Lemaitre, J. and Chaboche, J.-L. (1978). Aspect phénoménologique de la rupture par endommagement. *J. Méc. Appl.* **2,** 317–365.

Lemaitre, J. and Chaboche, J.-L. (1985). *Mécanique des Matériaux Solides*. Dunod, Paris.

Love, A. E. H. (1927). *The Mathematical Theory of Elasticity*. Cambridge University Press, Cambridge.

Marshall, D. B. and Oliver, W. C. (1987). Measurement of interfacial mechanical properties in fiber-reinforced ceramic composites. *J. Am. Ceram. Soc.* **70,** 542–548.

McMeeking, R. M. and Evans, A. G. (1900). Matrix fatigue cracking in fiber composites. *Mech. Mater.* **9,** 217–227.

Pryce, A. W. and Smith, P. A. (1992). Modelling of the stress/strain behavior of unidirectional ceramic matrix composite laminates. *J. Mater. Sci.* **27,** 2695–2704.

Rabotnov, Y. N. (1963). On the equations of state for creep. In *Progress in Applied Mechanics, Prager Anniversary Volume* (Edited by W. T. Koiter), pp. 307–315. Macmillan, New York.

Sherman, D. (1992). The mechanical behavior of brittle ductile laminated system. Ph.D. dissertation, University of California, Santa Barbara, CA.

Volterra, V. (1907). Sur l'équilibre des corps élastiques multiplement connexes. *Ann. Scient. de l'Ecole Normale Supérieure, Paris* **24,** 401–518.

APPENDIX

To compute the elastic energy due to slip with no external stress, one needs to compute the strain contribution of the opening displacement due to slip Δ_s in parts (1) and (2) over a slip length l_F:

$$\delta\varepsilon_1(z) = \begin{cases} -\dfrac{(1-f)E_2}{fE_1}\delta\varepsilon_2 F(z) & \text{if } 0 < z < l_F \\ 0 & \text{if } l_F < z < L \end{cases} \tag{A1a}$$

$$\delta\varepsilon_2(z) = \begin{cases} \delta\varepsilon_2 F(z) & \text{if } 0 < z < l_F \\ 0 & \text{if } l_F < z < L. \end{cases} \tag{A1b}$$

The opening displacement due to slip Δ_s can be related to the previous quantities by

$$\Delta_s = \int_0^{l_f} (\delta\varepsilon_2(z) - \delta\varepsilon_1(z))\,dz = \frac{E\delta\varepsilon_2}{fE_1} l_F \bar{F}. \tag{A2}$$

The overall inelastic strain due to slip is given by the average displacement of the unbroken layer (2):

$$\alpha = \frac{1}{L}\int_0^{l_F} \delta\varepsilon_2(z)\,dz = \frac{l_F}{L}\delta\varepsilon_2 \bar{F} \tag{A3}$$

and the corresponding elastic energy is written as

$$\psi_s = \frac{1}{L}\int_0^{l_f} \tfrac{1}{2}[fE_1\delta\varepsilon_1^2(z) + (1-f)E_2\delta\varepsilon_2^2(z)]\,dz = \frac{E\delta\varepsilon_2^2 l_F}{2}\frac{l_F}{L}\frac{(1-f)E_2}{fE_1}\bar{F}. \tag{A4}$$